Environ. Eng. Res. Vol. 7, No. 2, pp. 103~111. 2002
Korean Society of Environmental Engineers

URANIUM(VI) ADSORPTION AND TRANSPORT IN CRUSHED GRANITE

Dong-Kwon Keum†, Byung-Jae Choi, Min-Hoon Baik, and Pil-Soo Hahn
Korea Atomic Energy Research Institute, Daejeon 305-390, Korea
(received February 2002, accepted June 2002)

Abstract : The adsorption and transport characteristics of uranium (VI) by using a crushed-granite of Korean origin were investigated to better identify the adsorption processes involved and to obtain suitable data for models describing the uranium transport in the granite. In order to obtain the batch K_d and the breakthrough curve of uranium, experiments were conducted with both batch and column systems under the conditions of varying pH and temperature. Model prediction for the uranium transport was performed with the plate model of chromatography combined with two adsorption models: the equilibrium adsorption model and the kinetic adsorption model.

The batch K_d was increased with temperature, indicating that the uranium adsorption onto the granite was endothermic. The pH dependency of the K_d showed a typical adsorption characteristic of actinides onto constituent mineral of geological media, which showed very strong adsorption in the range of pH 6~7. The uranium transport data was well described by the linear kinetic transport model. The result indicated that the uranium adsorption process was time-dependent, rather than in equilibrium during the migration in the column. The column K_d was much larger than the batch K_d at the same total concentration and pH.

Key Words : adsorption, granite, kinetic transport model, transport, uranium

INTRODUCTION

The safe disposal of high-level radioactive wastes (HLW) is a crucial step of the nuclear fuel cycle. The most widely accepted solution for the disposal of HLW is the construction of underground repository to accommodate waste packages.[1] In this case, the most probable escape pathway for radionuclides from a repository to the biosphere is via water-bearing fractures in surrounding rock. A safety assessment for such a disposal requires the knowledge of the dynamics of groundwater flow and of role of the surrounding geological body for ensuring an adequate nuclide containment.

The radionuclide transport through geologic media is strongly influenced by sorption onto surrounding rock and mineral phases. The sorption process is dependent on various geochemical parameters, including aqueous properties, sorptive properties as well as temperature and redox potentials. Such a complexity of sorption process in natural system makes it difficult to describe and predict radionuclide retardation and transport in geochemical systems of variable mineralogic composition and changing aqueous speciation. Although a surface complexation model can deal with the dependency of chemical conditions, especially the pH and concentrations of complexing ligands, on adsorption of radionuclide onto mineral,[2~6] the model is yet impractical to the safety assessment due to

†Corresponding author
E-mail: dkkeum@kaeri.re.kr
Tel: +82-42-868-2058, Fax: +82-42-868-8850

the uncertainty and lack of data available.[7] At the present exercise of safety assessment, sorption process is mostly described in terms of an empirical distribution coefficient (K_d), expressed as concentration ratio of radionuclide between water and solid surface. The value of K_d is normally measured by batch (static) method for a specified condition. However, flow-through column experiment,[8~12] together with the batch experiment for K_d measurement, is also important to examining how adsorption influences radionuclide migration.

In this study, uranium(VI) is used to investigate actinide transport in domestic granite, which is potential bedrock for deep geological disposal of HLW in Korea. The purposes of this paper are to improve our understanding of the uranium migration in domestic granite, to compare the batch and column K_d, and to obtain suitable data for a transport model to describe the movement of U(VI).

MODEL

The surface environment can be regarded as giant chromatography systems with porous media as the solid phase and groundwater as the carrier. Depending on the groundwater flow concept applied, transport model can be classified into two types: a continuous model and a discrete mixing cell model. The continuous model assumes continuous spatial variations in solute concentrations. The discrete model uses a network of suitably connected subsystems, each one having its own properties, to represent spatial variations. The basic subsystem of discrete model is mixing cell of uniform concentration. In face of the difference of the hydrological transport concept, the two models produce same prediction results at broad conditions.[13]

The plate theory of chromatography or mixing cell concept has been often applied to predict the movement of reactive and non-reactive solute in soil and groundwater.[14,15] According to the plate theory, the chromatographic column is mathematically equivalent to a plate column where the total length is divided into N_c plates (Figure 1). A differential material balance on solute around plate n gives

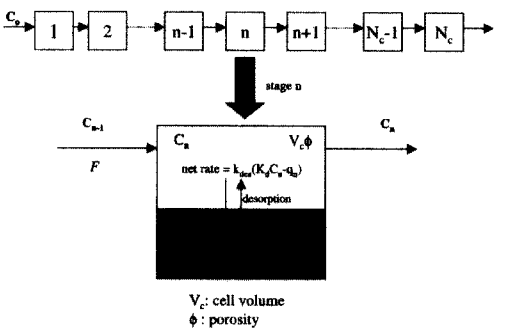

Figure 1. Concept of plate model of chromatography.

$$\frac{F}{V_c}(C_{n-1}-C_n)dt = d[\phi C_n + \rho_p(1-\phi)q_n], \quad n=1,2,\ldots N_c \tag{1}$$

where F is the mobile phase flow rate, C_n and C_{n-1} the mobile phase concentration of plate n and n-1, respectively, q_n the adsorbed phase concentration of plate n, V_c the volume of plate n, ϕ the column porosity, and ρ_p the particle density.

The first order linear kinetic adsorption model assumes that the sorption rates are to be first order with respect to the mobile and adsorbed phase concentration, respectively.

$$\frac{dq_n}{dt} = k_{des}(K_d C_n - q_n), \quad n=1,2,\ldots N_c \tag{2}$$

In the case of the equilibrium adsorption model, the adsorption rate is equal to the desorption rate. There is no net change in q_n and C_n. Thus, as q_n is no longer a function of time under equilibrium conditions, the left side of Equation (2) is zero and the equation lead to

$$q_n = K_d C_n, \quad n=1,2,\ldots N_c \tag{3}$$

For initial and boundary conditions, it is assumed that the mobile phase enters plate 1

with a solute concentration of C_o but all the plates at the start are solute free so that

$$B.C.;\ C_o = constant \tag{4}$$

$$I.C.;\ C_1^o = C_2^o = \ldots\ldots = C_{N_c}^o = 0,$$
$$q_1^o = q_2^o = \ldots\ldots = q_{N_c}^o = 0 \tag{5}$$

From the above model we can see that the kinetic transport model consists of $2N_c$ ordinary differential equations with four parameters (k_{des}, K_d, N_c, ϕ), while the equilibrium transport model is given by N_c ordinary differential equations with three parameters (K_d, N_c, ϕ). In the case of the equilibrium transport model the concentration of solute in the plate N_c can be analytically derived.[16]

$$C_{N_c}(t) = C_o\left(1 - \sum_{r=0}^{N_c-1} \frac{(t/t_o)^r}{r!} e^{-t/t_o}\right) \tag{6}$$

where t_o is the mean residence time of tracer in a plate, which is defined by $t_o = RL/UN_c$ where L is the total column length, U the velocity of mobile phase in column, and R the retardation factor given by $R = 1 + (1-\phi)\rho_p K_d/\phi$.

EXPERIMENTALS

Materials

Crushed granite was prepared by sieving after crushing the granite block quarried from a domestic site (Eyjungbu, Gyeonggi-do). The particle diameter is ranged between 0.021 cm and 0.03 cm and the surface area measured by BET (N_2 adsorption) is 1.0 m^2/g. A suitable amount of the crushed granite was sufficiently washed in acidic solution to remove impurities and organics. After the washing the crushed granite was smoothly dried at about 40℃ in an oven. Uranium nitrate ($UO_2(NO_3)_2 \cdot 6H_2O$) and ultra pure water were used to make the uranium solution. The ionic strength of the solution was adjusted to 0.01 M with $NaClO_4$ all through experiments.

Experimental Method

Batch adsorption experiments were conducted in a temperature controlled incubator shaker without attempting to exclude air. The solid to liquid ratios was fixed at 250 g/L. The 25 g of adsorbent were added to 0.1 liter $NaClO_4$ (0.01 M) solution in PMP (poly methyl propylene) flask. The suitable amount of uranium nitrate was then added to the solution to adjust the initial concentration, and the pH was checked and adjusted if necessary to the prefixed value. After the reaction the final pH was measured, and two phases were separated by membrane filter with the pore size of 0.2 μm. The solution passed through the filter was analyzed for the uranium concentration by the ICP-MS (Ultramass 700).

Figure 2 shows the schematic column experimental system. The chromatographic column was made of a Pyrex tube with water jacket, 31 cm in length and 1 cm in inside diameter. The column was connected to a HPLC pump and to a conductivity cell or a fractional collector. A three-way valve was installed at the column inlet, allowing the column to be washed out when an abrupt composition change was performed. The dead volume (6.48 mL) in the connecting tube was determined by the retention time of the bromide peak measured by directly connecting the inlet tube and the outlet tube of the column. Temperature was controlled by circulating water from the water-bath equipped with

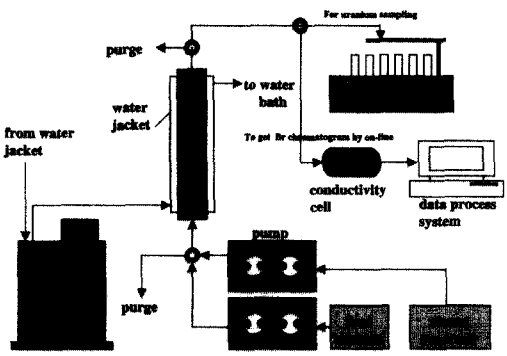

Figure 2. Schematic diagram of column experimental system.

temperature controller. The bromide chromatogram was obtained with varying flow rate. The bromide concentration at the column outlet was continuously measured using the ion-conductivity meter in order to obtain the chromatogram. In the uranium transport experiment, the flow rate was fixed to 60 mL/h. The uranium solution at the column outlet was sampled using the fractional collector, and the concentration was analyzed by the ICP-MS.

RESULTS AND DISCUSSION

Uranium Adsorption in Batch Experiment

The formation of precipitates of adsorbing components during the adsorption experiment produces the confounding and biasing results on the adsorption.[7] We first evaluated the solubility of uranium as a function of pH using the geochemical code MUGREM[17] and the thermodynamic data.[18] In the calculation, the hydroxyl as well as the carbonate complex of uranium was considered because the experiment was conducted with the distilled water without attempting to exclude air. The schoepite ($UO_3 \cdot 2H_2O$) was assumed to be the solubility-limiting solid phase. The calculation result revealed that the solubility was a minimum (about 2×10^{-5} M) at near the pH 6. In order to experimentally check the possibility of uranium precipitation, we performed the blank test without adsorbent with solution of concentration of 10^{-5} M. As a result, no difference in concentration was found between after and before filtration of solution in the blank experiment. Accordingly, all the batch adsorption experiments were conducted with the total uranium concentration of 10^{-5} M.

Figure 3 and Table 1 show the percent adsorbed amount and static K_d values of uranium with varying pH and temperature, respectively. Uranium sorption starts to increase at the weak acidic conditions and is a maximum at near neutral pH (6~7) and decreases sharply toward alkaline conditions. The increase in the uranium adsorption at the acidic pH is due to the increase in the uranium hydroxyl strongly adsorbed in this pH range. The decrease in the uranium adsorption at the alkaline pH is ascribed to the increase in aqueous uranium carbonate complexes with increasing pH.[4] This sharp decrease in uranium sorption in the alkaline conditions is generally not observed in the carbonate-free systems.[19,20] The pH dependency of uranium adsorption on granite is very similar to the metal adsorption onto minerals such as goethite, hematite and so on, which shows very strong adsorption in the pH range of 6~7. On the other hand, the increase in temperature enhances the uranium adsorption on granite. This indicates that uranium adsorption reaction onto the granite is endothermic.

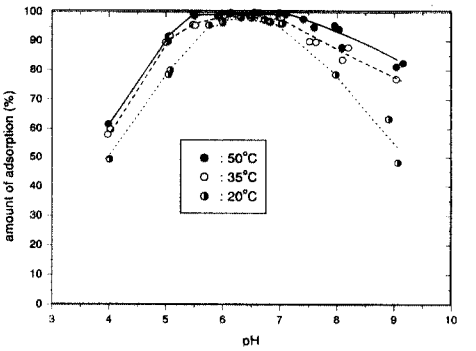

Figure 3. Percent adsorbed amount of uranium measured from the batch experiment under varying pH and temperature (total uranium concentration=10^{-5} M, ionic strength=0.01 M, ratio of solid to solution=250 g/L).

Table 1. The K_d[a] values estimated from the batch experiment

Temperature (℃)	pH					
	4	5	6	7	8	9
20	3.8	13.4	107.3	104.1	14.7	6.5
35	5.6	32.4	292.3	258.0	26.8	14.2
50	6.4	40.4	396.0	1996.0	71.5	22.7

a) K_d(mL/g)={%ads/(100-%ads)} × W(solid concentration)

Column Characteristics

The measurement of breakthrough of non-

sorbing tracer allows the measurement of the flow characteristics of column such as porosity and axial dispersion. In the plate model of chromatography, the number of cell (N_c) accounts for the extent of axial dispersion. If a pulse of bromide is added at the inlet of a column, the retention time and the dispersivity of chromatogram at the column outlet are determined by the extent of porosity and the axial dispersion. We estimated N_c and porosity (ϕ) as fitting parameters from the bromide chromatogram by the Marquardt algorithm.[21] The porosity was estimated to be 0.50 ± 0.01, which was independent of flow rate. This value of the porosity agreed well with that estimated by using the particle density (2.55 g/cm^3) and the weight of the crushed granite packed in the column. Table 2 shows N_c values calculated with varying flow rate. The values increase with decreasing flow rate. The larger the flow rate is, the greater dispersive flow is resulted in within the range of the studied flow rate. According to Sardin and Schweich,[13] the number of cell in the plate model of chromatography corresponds to the Peclet number (Pe) of the continuous model, and both models lead to almost the same results if $Pe(>10)$ is equal to $2N_c$. We also confirmed no difference of calculation result between the two models when $Pe=2N_c$. The Peclet numbers reduced from the relationship are in the range of 180 to 250. These values of Pe reveal small dispersive flow. On the other hand, Figure 4 shows the comparison of the experimental bromide chromatogram with the equilibrium transport model without adsorption ($K_d=0$). The very good agreement between the model prediction and the experimental data proves that no kinetic limitation to diffusional mass transfer around or inside the granite particles occurs in the conditions chosen for the experiment.

Table 2. The number of cell and Peclet number obtained from the chromatogram of bromide

Flow rate (mL/h)	N_c	Pe*
30	126	252
45	119	238
60	93	186
75	90	180

* $Pe=2N_c$

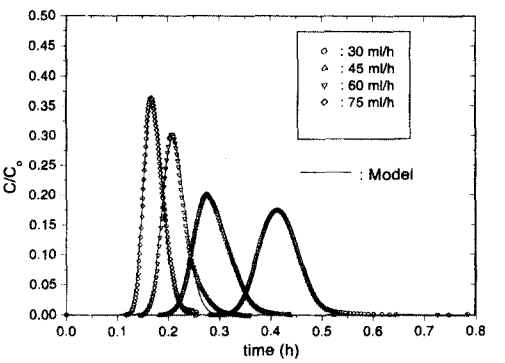

Figure 4. Comparison of the experimental data with the model calculation for the bromide transport.

Sensitivity of N_c and k_{des} on Breakthrough Curve

The retention time of the breakthrough curve of adsorbing solute is determined by the value of K_d, while the dispersivity is controlled by both the rate constant of sorption (k_{des}) and the number of cell (N_c) when no other process such as intraparticle diffusion is involved. The sensitivity analysis of N_c and k_{des} on the breakthrough curve of adsorbing solute is therefore necessary to understand the relative importance of those two processes on the dispersivity of the curve. Figure 5 shows the breakthrough curves calculated with varying N_c and k_{des}. The model prediction was numerically obtained by the IMSL subroutine DIVPAG, which uses the Gear algorithm with variable step size.[22] When the value of k_{des} approaches to infinite (the equilibrium case), only the N_c, which accounts for the extent of axial dispersion, is responsible for the dispersivity of the breakthrough curves. The breakthrough curve becomes steeper with increasing the number of cell (Figure 5(a)). The effect of dispersion begins to decrease with increasing

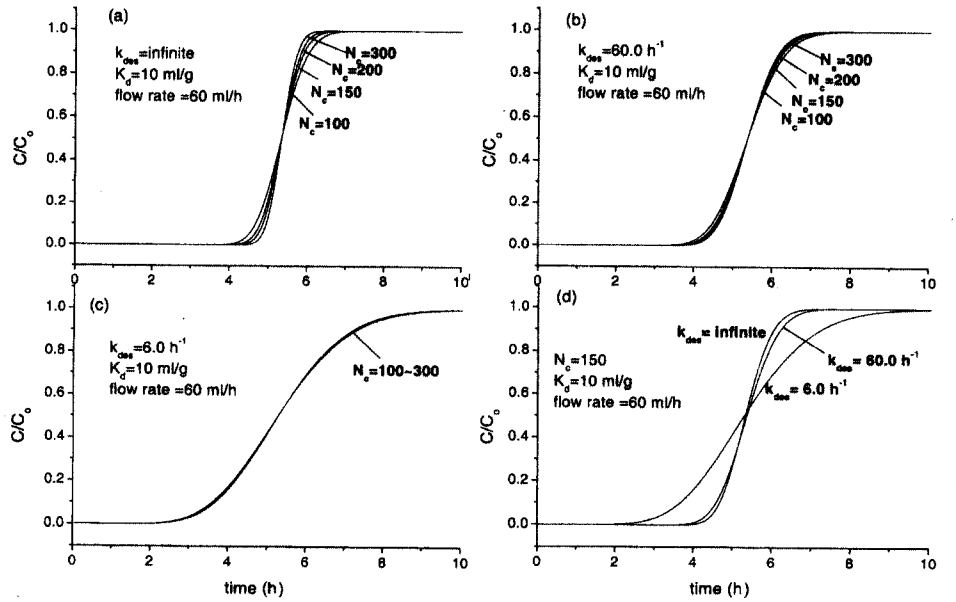

Figure 5. Sensitivity of N_c and k_{des} on the dispersivity of the uranium breakthrough curve.

kinetic effect (decreasing sorption rate). At the low value of adsorption rate constant the dispersion effect appears to be negligibly small, and the dispersion effect is no longer a significant factor on the transport of uranium (Figure 5(c)). At constant N_c, the dispersivity of breakthrough curve is only affected by the sorption rate constant. The more dispersive breakthrough curve is produced with the less value of sorption rate constant (Figure 5(d)). In this case, the rate constant is the only fitting parameter to adjust the dispersivity of the experimental breakthrough curve.

Transport of Uranium in Column

In this study, the uranium transport experiments at pH 4 where a week adsorption of uranium is expected were performed to obtain breakthrough curves within a reasonable experimental time. Figure 6 shows the experimental breakthrough curves of uranium measured with different temperature. The increase in temperature produces delayed breakthrough time, which is consistent with the temperature effect obtained by the batch experiment; the batch K_d was increased with temperature. Under the present experimental conditions, the uranium seems to be fully recovered in the elution stage, indicating the reversible adsorption of uranium.

From the comparison of the model prediction with the experimental data of uranium transport, we can see that the equilibrium transport model is unable to describe the experimental data. The curve predicted by the equilibrium model with the batch K_d elutes much earlier and shows steeper rising than the experimental curve. The equilibrium model with the column K_d has a retention time similar to the experimental curve but produces steeper rising and sharper decreasing breakthrough curve. The equilibrium transport model may give a good match with the experimental curve if two parameters (K_d and N_c) are used as fitting parameters. However, the extent of axial dispersion is generally not a fitting parameter for the breakthrough curve of adsorbing solute because the axial dispersion is independent of the sorption effect, and thus it should be determined from a separate experiment using non-adsorbing tracer to prevent the misleading of the result due to the sorption. In this study N_c was estimated from the chromatogram of the bromide (Table 2). The discrepancies between

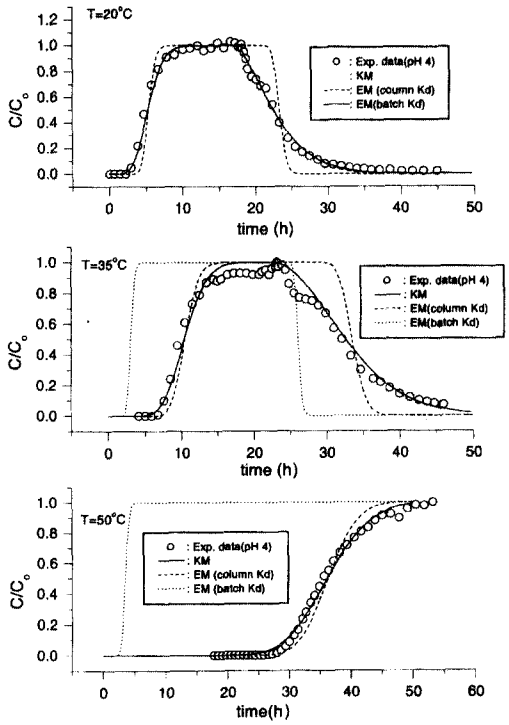

Figure 6. Comparison of the experimental data with the model predictions for the uranium transport.

the equilibrium transport model and the experimental curve imply that the uranium adsorption process is time-dependent and needs a finite time to reach equilibrium. This result seems to be caused by the relatively large convective flow rate, compared to the sorption rate. On the other hand, the experimental curves show an asymmetrical shape. It indicates that the sorption rate during the loading step is different from that during the elution step. Hence we have applied different values of the adsorption rate constant for the front zone and the trailing zone of the experimental curve, respectively. The calculated result is shown in Table 3. For the elution step the adsorption rate constant is smaller than that for the loading step. It reveals that desorption rate is slower in the course of the elution step. Meanwhile, no difference is found between the K_d values obtained by the equilibrium transport model and the kinetic transport model. It is because the K_d is responsible only for the retention time of breakthrough curve and does not affect the dispersivity of the curve. From comparing the column and the batch K_d value, we can see that the column K_d is much larger than the batch K_d at the same total uranium concentration and pH. The difference is possibly due to the different ratio of solid to solution volume between the batch and the column experiment.

CONCLUSION

The adsorption and transport of uranium (VI) was investigated with a series of batch and column experiments using the granite sampled from Eyjungbu, Gyeonggi-do, Korea. The batch K_d and the breakthrough curve of uranium were obtained under the conditions of varying pH and temperature. Model prediction for uranium transport was performed with the plate model of chromatography combined with two different adsorption models: the equilibrium adsorption model and the kinetic adsorption model.

The batch K_d was increased with temperature, indicating that the uranium adsorption onto the granite was endothermic. The pH

Table 3. Experimental conditions and fitting parameters obtained from the column experiment of uranium

Loading time (h)	pH	Temp. (℃)	Equilibrium model (EM)		Kinetic adsorption model (KM)		
			Batch K_d (mL/g)	Column K_d (mL/g)	K_d (mL/g)	k^f_{des} (h^{-1})	k^r_{des} (h^{-1})
18	4	20	3.8	10.0	10.0	4.2	0.60
23	4	35	5.6	20.0	20.0	4.2	0.54
step	4	50	6.4	70.0	70.0	4.2	-

dependency of the K_d showed a typical adsorption characteristic of actinides onto constituent minerals of geological media, which showed very strong adsorption in the range of pH 6~7. The experimental breakthrough curves of uranium exhibited the kinetic adsorption characteristics during the migration in the column. The significance of this result lies in that the local equilibrium assumption of adsorption is not always true in the transport of uranium. The kinetic adsorption model may be necessary for the modeling of uranium transport under the condition where the adsorption rate is not sufficiently high, compared to the mobile phase velocity. However, the column K_d obtained from the transport data of the uranium was independent of the adsorption model applied. This result is ascribed to the fact that the equilibrium state approaches to the same conditions given the total concentration, pH and temperature. The column K_d was much larger than the batch K_d, which is likely to be attributed to the larger solid to liquid volume ratio of the column system.

ACKNOWLEDGEMENT

This work was supported by the Nuclear Research program of MOST, Korea

REFERENCES

1. OECD/NEA, Geological disposal of radioactive waste: An overview of the current status of understanding and development, OECD, February (1984).
2. Arnold, T., Zorn, T., Zänker, H., Bernhard, G., and Nitsche, H., "Sorption behavior of U(VI) on phyllite: experiments and modeling," *J. Contam. Hydrol.*, **47**, 219~231 (2001).
3. Prikryl, J. D., Jain, A., Turner, D. R., and pabalan, R. T., "Uranium sorption behavior on silicate mineral mixtures," *J. Contam. Hydrol.*, **47**, 241~253, (2001).
4. Pabalan, R. T., Turner, D. R., Bertetti, F. P., and Prikryl, J. D., "Uranium(VI) sorption onto selected mineral surface," *Adsorption of Metals by Geomedia*, Jenne, E. A.(Ed.), Academic Press, San Diego, pp. 99~130 (1998).
5. Waite, T. D., Davis, J. A., Payne, T. E., Waychunas, G. A., and Xu, N., "Uranium(VI) adsorption to ferrihydrite: application of a surface complexation model," *Geochim. Cosmochim. Acta*, **58**, 5465~5478 (1994).
6. Dzombak, D. A. and Morel, F. M. M., Surface complexation modeling: Hydrous Ferric oxide, John Wiley & Sons, Inc., New York (1990).
7. Serne, R. J., "Conceptual adsorption models and open issues pertaining to performance assessment," *Proceedings of an NEA Workshop on Radionuclide sorption from the safety evaluation perspective* OECD, Paris, pp. 237~282 (1992).
8. Kohler, M., Curtis, G. P., Kent, D. B., and Davis, J. A., "Experimental investigation and modeling of uranium (VI) transport under variable chemical conditions," *Water Resour. Res.*, **32**, 3539~3551 (1996).
9. Read, D., Lawless, T. A., Sims, R. J., and Butter, K. R., "Uranium migration through intact sandstone cores," *J. Contam. Hydrol.*, **13**, 277~289 (1993).
10. Silva, R. J., "Mechanisms for the retardation of uranium (VI) migration," *Mat. Res. Soc. Symp. Proc.*, **257**, 323~330 (1992).
11. Cui, D. and Eriksen, T., "Reactive transport of Sr, Cs and Tc through a column packed with fracture filling material," *Radiochim. Acta*, **82**, 287~292 (1998).
12. Bidoglio, G., Offermann, P., and Saltelli, A., "Neptunium migration in oxidizing clayey sand," *Appl. Geochem.*, **2**, 275~284 (1987).
13. Sardin, M. and Schweich, D., "Modeling the nonequilibrium transport of linearly interacting solutes in porous media: A review," *Water Resour. Res.*, **27**, 2287~2307 (1991).
14. Bajracharya, K. and Barry, D. A., "Mixing

cell models for nonlinear equilibrium single species adsorption and transport," *J. Contam. Hydrol.*, **12**, 227~243 (1993).
15. Jauzein, M., Andre, C., Margrita, R., Sardin, M., and Schweich, D., "A flexible computer code for modeling transport in porous media," *Impact. Geoderma*, **44**, 95~113 (1989).
16. Said, A. S., "Theory and mathematics of chromatography," *Chromatographic method*, Bertsch, W. et al., (eds.), Dr. Alfred Huthig Verlag Heidelberg, pp. 127~128 (1981).
17. Keum, D. K. and Hahn, P. S., "Application and development of a multigeochemical reaction equilibrium model (MUGREM)," *Environ. Eng. Res.*, **4**, 113~126 (1999).
18. Grenthe, I., Fuger, J., Konings, R. J. M., Lemire, R. J., Muller, A. B., Nguyen-Trung, C., and Wanner, H., Chemical Thermodynamics 1: Chemical Thermodynamics of Uranium, OECD/BEA, North-Holland, Elsevier Scientific Publishing Co. New York (1992).
19. McKinley, J. P., Zachara, J. M., Smith, S. C., and Turner, G. D., "The influence of hydrolysis and multiple site-binding reactions on adsorption of U(VI) to montmorillonite," *Calys Clay Miner.*, **34**, 586~598 (1995).
20. Turner, G. D., Zachara, J. M., Mckinley, J. P., and Smith, S. C., "Surface-charge properties and UO_2^{2+} adsorption of a surface smectite," *Geochim. Cosmochim. Acta*, **60**, 3399~3414 (1996).
21. Kuester, J. L. and Mize, J. H. Optimization techniques with Fortran, McGraw-Hill, New York, pp. 240~250 (1973).
22. Digital Visual Fortran, IMSL(R) Fortran 90 MP Library, Visual Numerics, Inc. (1997).